



**HAL**  
open science

## **S-5P/TROPOMI-Derived NO<sub>x</sub> Emissions From Copper/Cobalt Mining and Other Industrial Activities in the Copperbelt (Democratic Republic of Congo and Zambia)**

S. Martínez-Alonso, J. Veefkind, B. Dix, B. Gaubert, N. Theys, Claire  
Granier, A. Soulié, S. Darras, H. Eskes, W. Tang, et al.

### ► To cite this version:

S. Martínez-Alonso, J. Veefkind, B. Dix, B. Gaubert, N. Theys, et al.. S-5P/TROPOMI-Derived NO<sub>x</sub> Emissions From Copper/Cobalt Mining and Other Industrial Activities in the Copperbelt (Democratic Republic of Congo and Zambia). *Geophysical Research Letters*, 2023, 50 (19), 10.1029/2023GL104109 . hal-04794013

**HAL Id: hal-04794013**

**<https://hal.science/hal-04794013v1>**

Submitted on 21 Nov 2024

**HAL** is a multi-disciplinary open access archive for the deposit and dissemination of scientific research documents, whether they are published or not. The documents may come from teaching and research institutions in France or abroad, or from public or private research centers.

L'archive ouverte pluridisciplinaire **HAL**, est destinée au dépôt et à la diffusion de documents scientifiques de niveau recherche, publiés ou non, émanant des établissements d'enseignement et de recherche français ou étrangers, des laboratoires publics ou privés.



Distributed under a Creative Commons Attribution - NonCommercial - ShareAlike 4.0 International License

# Geophysical Research Letters<sup>®</sup>



## RESEARCH LETTER

10.1029/2023GL104109

### Key Points:

- We quantified annual TROPOspheric Monitoring Instrument (TROPOMI)-derived NO<sub>x</sub> emissions from point sources corresponding to copper/cobalt mines, despite high background values
- Annual emissions from individual point sources are strongly correlated with annual production from colocated single mines, one oil refinery
- TROPOMI is relevant to monitoring air quality and mining/industrial production in remote regions where these activities are growing rapidly

### Supporting Information:

Supporting Information may be found in the online version of this article.

### Correspondence to:






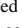

S. Martínez-Alonso,  
[sma@ucar.edu](mailto:sma@ucar.edu)

### Citation:

Martínez-Alonso, S., Veeffkind, J. P., Dix, B., Gaubert, B., Theys, N., Granier, C., et al. (2023). S-5P/TROPOMI-derived NO<sub>x</sub> emissions from copper/cobalt mining and other industrial activities in the Copperbelt (Democratic Republic of Congo and Zambia). *Geophysical Research Letters*, 50, e2023GL104109. <https://doi.org/10.1029/2023GL104109>

Received 19 APR 2023  
Accepted 25 AUG 2023

## S-5P/TROPOMI-Derived NO<sub>x</sub> Emissions From Copper/Cobalt Mining and Other Industrial Activities in the Copperbelt (Democratic Republic of Congo and Zambia)

S. Martínez-Alonso<sup>1</sup> , J. P. Veeffkind<sup>2,3</sup>, B. Dix<sup>4</sup> , B. Gaubert<sup>1</sup> , N. Theys<sup>5</sup>, C. Granier<sup>4,6,7</sup> , A. Soulié<sup>6</sup>, S. Darras<sup>8</sup>, H. Eskes<sup>2</sup>, W. Tang<sup>1</sup> , H. Worden<sup>1</sup> , J. de Gouw<sup>4,9</sup> , and P. F. Levelt<sup>1,2,3</sup>

<sup>1</sup>Atmospheric Chemistry Observations and Modeling Laboratory, National Center for Atmospheric Research, Boulder, CO, USA, <sup>2</sup>Royal Netherlands Meteorological Institute, De Bilt, The Netherlands, <sup>3</sup>Department of Civil Engineering and Geosciences, Technical University of Delft, Delft, The Netherlands, <sup>4</sup>Cooperative Institute for Research in Environmental Sciences, University of Colorado Boulder, Boulder, CO, USA, <sup>5</sup>Royal Belgian Institute for Space Aeronomy (BIRA-IASB), Brussels, Belgium, <sup>6</sup>Laboratoire d'Aérodynamique, CNRS, University of Toulouse UPS, Toulouse, France, <sup>7</sup>Chemical Sciences Laboratory, National Oceanic and Atmospheric Administration, Boulder, CO, USA, <sup>8</sup>Observatoire Midi-Pyrénées, Toulouse, France, <sup>9</sup>Department of Chemistry, University of Colorado Boulder, Boulder, CO, USA

**Abstract** We have analyzed Sentinel-5 Precursor TROPOspheric Monitoring Instrument (TROPOMI) data over the Copperbelt mining region (Democratic Republic of Congo and Zambia). Despite high background values, annual 2019–2022 means of TROPOMI NO<sub>2</sub> (nitrogen dioxide) show local enhancements consistent with six point sources (four copper/cobalt mines, two cities) where high-emission industrial activities take place. We have quantified annual NO<sub>x</sub> (nitrogen oxides) emissions from these point sources, identified temporal trends in emissions, and found strong correlations with production data from colocated mines and one oil refinery. The Copernicus Atmosphere Monitoring Service Global Anthropogenic (CAMS-GLOB-ANT) version 5 inventory underpredicts TROPOMI-derived emissions and lacks the temporal trends observed in TROPOMI and mine/refinery production. These results demonstrate the potential for satellite monitoring of mining and other industrial activities, often unreported or underestimated, which impact the air quality of local communities. This is particularly important for Africa, where mining is increasing aggressively.

**Plain Language Summary** We show for the first time that annual NO<sub>x</sub> gas pollution emitted by individual copper/cobalt mines can be measured with TROPOMI satellite data, even in the presence of high background pollution from biomass burning and other sources. This is important for monitoring the air quality of local communities, particularly when these industrial activities proliferate in close proximity to population centers (as is the case in the Copperbelt mining region and in other African regions) and without sufficient ground measurements of air pollution levels. Additionally, we show for the first time that the annual amount of NO<sub>x</sub> pollution emitted by these single point sources is strongly correlated with annual production from individual, colocated copper/cobalt mines and one oil refinery. Studies like this can be used to estimate mine/oil refinery production before companies release their annual reports or (for non-publicly traded companies) in the absence of such reports. Insufficient emissions from mines claiming high production could indicate production from a different source. Joint analysis of satellite-derived emissions and mine production reports could be useful in improving the traceability of minerals extracted in conflict areas.

## 1. Introduction

The Copperbelt, a mining region straddling the Democratic Republic of Congo (DRC) and Zambia, is currently of great strategic interest because it is the world's largest cobalt producer and holds almost half of the world reserves (U.S. Geological Survey, 2022). Cobalt production in the Copperbelt (mostly in the DRC) has increased ~600% between 1990 and 2021 (U.S. Bureau of Mines, 1992; U.S. Geological Survey, 2022), driven by its use in lithium-ion batteries which power mobile phones, laptops, and electric cars. Access to the Copperbelt's cobalt is becoming a matter of national and global energy security (Gulley, 2022). Cobalt is, however, a byproduct of copper mining; copper is the main ore (by volume) extracted in the Copperbelt. Previous studies have documented the impact of cobalt and/or copper mining in the region's soils and water (Atibu et al., 2016), land use (Mwitwa et al., 2012), and neonatal health (Kayembe-Kitenge et al., 2019; Van Brusselen et al., 2020). The impact on local air quality remained unknown. Here we quantify the effect of increasing mining activity on

© 2023. The Authors.

This is an open access article under the terms of the [Creative Commons Attribution-NonCommercial-NoDerivs License](https://creativecommons.org/licenses/by/4.0/), which permits use and distribution in any medium, provided the original work is properly cited, the use is non-commercial and no modifications or adaptations are made.

the air quality of this region using Tropospheric Monitoring Instrument (TROPOMI) satellite measurements (Veefkind et al., 2012) of NO<sub>2</sub> (nitrogen dioxide); TROPOMI SO<sub>2</sub> (sulfur dioxide) is also analyzed. Both gases are atmospheric pollutants (World Health Organization, 2021) relevant to air quality monitoring and forecasting. They are also considered short-lived climate forcers, important for understanding climate (Myhre et al., 2013).

NO<sub>x</sub> (NO<sub>2</sub> + NO, two nitrogen oxide species closely intertwined by oxidation and reduction reactions), has both anthropogenic (fossil fuel combustion, biomass burning) and natural (microbial activity in soils, lightning, wildfires) sources. Mining-related NO<sub>x</sub> is produced by high-temperature combustion of fuel used by trucks and other heavy machinery as well as by electric generators. The main sink of NO<sub>x</sub> is the hydroxyl radical (OH), with which it reacts within hours in the presence of light. NO<sub>x</sub> has a negative impact on air quality, both directly and as a precursor to tropospheric ozone and particulate matter. It is damaging to human health (affecting mostly the respiratory system) and crops, and contributes to the formation of smog and acid rain.

Measuring global and regional NO<sub>2</sub> was made possible by satellite instruments such as Global Ozone Monitoring Experiment (GOME), Scanning Imaging Absorption spectrometer for Atmospheric CHartographY (SCIAMACHY), Ozone Monitoring Instrument (OMI), and GOME-2 (Beirle et al., 2011; Leue et al., 2001; Richter et al., 2005, 2011). Labzovskii et al. (2022) reported regional-scale correlation between OMI NO<sub>2</sub> from heavy industry, including mining, and a coal production inter-annual variability index for the Siberian Kuzbass Basin. TROPOMI has allowed for the identification of NO<sub>2</sub> from cities (de Foy & Schauer, 2022; Goldberg et al., 2019; Pommier, 2022), power plants (Beirle et al., 2019, 2021; de Foy & Schauer, 2022; Goldberg et al., 2019), gas processing plants (Dix et al., 2022), and mines: gas and oil fields (Dix et al., 2020, 2022; Griffin et al., 2019), coal, copper, and gold mines (Goldberg et al., 2021).

SO<sub>2</sub> results from both anthropogenic (e.g., coal combustion, smelting of sulfur-rich ores) and natural (volcanism, marine biological processes) sources. It contributes to acid rain and particle formation. Exposure to SO<sub>2</sub> is harmful to human health, damages foliage, and impedes plant growth. Previous studies showed that SO<sub>2</sub> emissions could be estimated using satellite data from Total Ozone Mapping Spectrometer (TOMS), GOME, OMI, SCIAMACHY, and Ozone Mapping and Profiler Suite (OMPS) (Carn et al., 2007; Fioletov et al., 2013; Krueger, 1983; Zhang et al., 2017). Fioletov et al. (2020, 2023) reported TROPOMI-based emission estimates of SO<sub>2</sub> from power plants, volcanoes, oil and gas fields, and smelters.

We show that NO<sub>x</sub> emissions from copper/cobalt mining activities, among others, can be quantified based on TROPOMI data even in the presence of high background values from biomass burning and other sources (BIRA-IASB, 2021). Additionally, we identify inter-annual trends in TROPOMI-derived NO<sub>x</sub> emissions that are strongly correlated with mine and oil refinery production. Next we describe the data sets (Section 2) and methodology (Section 3) used in this study, we present our results (Section 4), discuss their relevance, and offer conclusions (Section 5).

## 2. Data Sets

TROPOMI, onboard the European Space Agency's Copernicus Sentinel-5 Precursor satellite (Veefkind et al., 2012), provides quasi-global daily coverage at high spatial resolution (3.5 × 5.5 km<sup>2</sup> for our species of interest). This is a nadir-viewing imaging spectrometer in a sun-synchronous orbit at 824 km of altitude, with 13:30 LST Equator-crossing time, and 2,600 km swath width. TROPOMI measures radiances in the ultraviolet, visible, and reflected infrared, from which concentrations of trace gases as well as cloud and aerosol properties are derived. Here we focus on TROPOMI measurements of tropospheric NO<sub>2</sub> and SO<sub>2</sub>, two pollutants produced by mining-related activities. NO<sub>2</sub> is retrieved from TROPOMI radiance measurements in the visible portion of the spectrum (400–496 nm) (Eskes & Eichmann, 2021; Eskes et al., 2022; van Geffen et al., 2020). We used daily TROPOMI NO<sub>2</sub> tropospheric column data from version 2 for the period between 1 January 2019 and 31 December 2022; this data set is consistent and, thus, apt for the analysis of temporal trends (Eskes et al., 2022). We also analyzed TROPOMI SO<sub>2</sub> data retrieved with COBRA, the Covariance-Based Retrieval Algorithm (Theys et al., 2021), from ultraviolet-visible radiances (310.5–326 nm) (Theys, 2022) for the 1 January 2019–31 July 2022 period; more recent data were unavailable at the time of writing.

Meteorological information needed to derive emissions from TROPOMI NO<sub>2</sub> vertical column density (VCD) was obtained from reanalysis data. By combining measurements and model results, reanalysis data sets provide consistent and gapless global coverage of essential climate variables. We used hourly ECMWF Reanalysis v5

(ERA5) data (Hersbach et al., 2020) provided at  $0.25^\circ \times 0.25^\circ$  resolution and generated by the Copernicus Climate Change Service at the European Center for Medium-Range Weather Forecasts.

Due to the unavailability of ground measurements, we compared inventory data to TROPOMI-derived  $\text{NO}_x$  emissions. Emission inventories are compilations of amounts of air pollutants released into the atmosphere, segregated by source and time period. We used Copernicus Atmosphere Monitoring Service Global Anthropogenic version 5 (CAM5-GLOB-ANT v5) emissions inventory data, an extension of version 4.2 (Granier et al., 2019), for 2019–2021 (“the inventory,” for simplicity); 2022 emissions were unavailable at the time of writing. We focused on monthly  $\text{NO}_x$  emissions, provided at  $0.1^\circ \times 0.1^\circ$  resolution.

Mine production data were obtained from the annual reports of publicly traded mining companies; these reports are mandated by official regulatory bodies such as the Securities and Exchange Commission in the United States and the Securities and Futures Commission in Hong Kong. Private mining companies are not required to disclose their production data. The specifics of the information available in these reports varies greatly: some companies only disclose amount of metal produced, while others offer additional relevant metrics such as amount of ore and waste mined, grade of ore processed, etc.

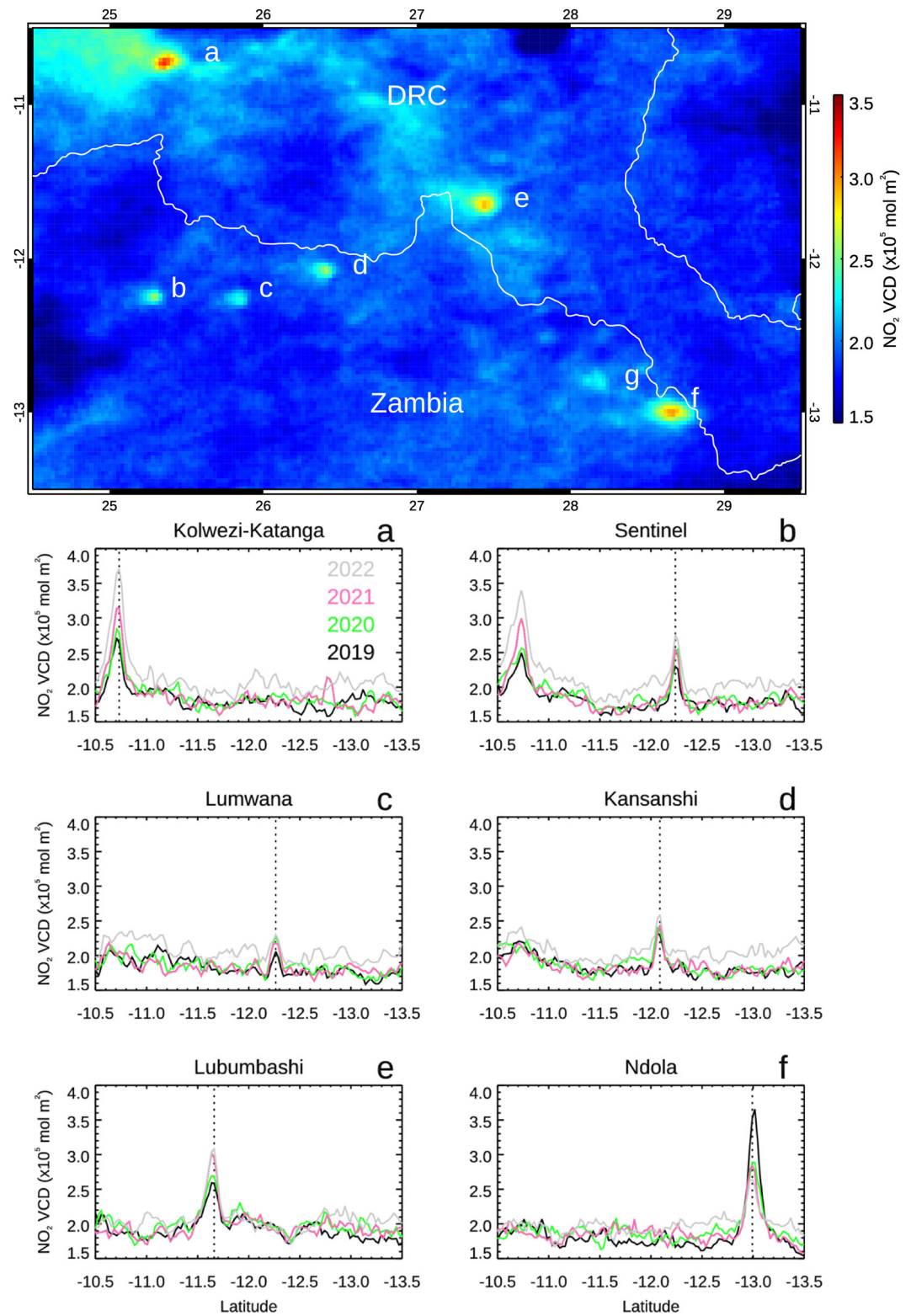
### 3. Methodology

To identify potential emission point sources such as mines, we produced annual means from daily TROPOMI  $\text{NO}_2$  VCD for the Copperbelt study area (Figure 1). Temporal averaging enhances the signal from constantly emitting sources while dampening more sporadic, background emissions from biomass burning, soils, and lightning.

Once the point sources were identified, we calculated daily TROPOMI-derived  $\text{NO}_x$  emissions for the study area using the divergence method (Beirle et al., 2019; Dix et al., 2022). This method derives emission based on a divergence term and a sink term, which account for wind dispersion effects and  $\text{NO}_x$  depletion by OH, respectively (Figure S1 in Supporting Information S1). The divergence method has been applied to quantify emissions from both areal (Dix et al., 2022) and point sources (Beirle et al., 2019, 2021; Dix et al., 2022), including cities (Beirle et al., 2021) and megacities (de Foy & Schauer, 2022). Applying the divergence method to areal sources should, however, be limited to instances where results are not dominated by the sink term. Dix et al. (2022) provide a detailed description with equations of the method as applied here. To calculate daily emissions we regridded daily VCD values to a common  $0.025^\circ \times 0.025^\circ$  grid. We filtered TROPOMI measurements to avoid clouds, errors, and problematic retrievals by using only those with quality assurance value  $\geq 0.75$  (Eskes et al., 2022); retrievals with solar zenith angle  $>60^\circ$  were rejected. Hourly values of fields (longitudinal and latitudinal horizontal wind at 100 m from the ground, pressure, and temperature) required for the emissions calculation were obtained from ERA5 reanalysis. All ERA5 fields were resampled to  $0.025^\circ \times 0.025^\circ$  spatial resolution and interpolated to the passing time of the closest (spatially and temporally) TROPOMI observation. Fields provided on pressure levels were interpolated to an altitude of 100 m above the ground. In our implementation, OH lifetime was calculated for each data point based on the solar zenith angle of the closest TROPOMI retrieval; Dix et al. (2022) used a constant solar zenith angle value over the area of interest at the overpass time. Daily emissions were averaged into annual means.

To calculate the actual  $\text{NO}_x$  emissions released from each point source, background values must be subtracted from the raw (non-background corrected) emissions. Several background removal approaches are possible. In their iterative peak fitting algorithm for the automatic detection of global  $\text{NO}_x$  point sources, Beirle et al. (2021) fitted a 2-D Gaussian on top of a linear background to each candidate point source. The parameters of the Gaussian were determined by least-squares fit of the result to the divergence values within 22 km around the candidate. Dix et al. (2022) removed from regional emissions (from both areal and point sources) a single background value determined by fitting a Gaussian curve to the left side of the histogram of emissions from an empirically chosen region. Our approach consisted of removing the local background values at each point source as follows. First we calculated the mean annual  $\text{NO}_x$  value per unit area of the local background: a  $1^\circ \times 1^\circ$  region surrounding each point source, excluding the point source plume. The location and extent of the point source plumes (Figure S2 in Supporting Information S1) were identified based on an empirical  $\text{NO}_x$  threshold ( $0.49 \text{ kg km}^{-2} \text{ hr}^{-1}$ ) obtained from mean raw emissions from the 2019–2022 period and found to minimize both false positives and false negatives. Annual means of background-removed emissions per surface area were then calculated for each point source plume by subtracting its mean background value from mean raw emission values. Background-removed emissions were integrated into a single value by accounting for the plume's areal extent.





**Figure 1.** (Top) 2019–2022 mean of TROPOMI NO<sub>2</sub> vertical column density (VCD) for the Copperbelt study region. Labels a through f show the six point sources analyzed. Label g shows Kitwe City. White lines indicate country borders. (bottom) Annual means of TROPOMI NO<sub>2</sub> VCD along latitudinal profiles centered at each of the six point sources, shown by vertical dotted lines. Labels as above. Profiles are color-coded according to year.

Dix et al. (2022) quantified systematic uncertainties due to variables used in the divergence method: background correction, wind level, wind data source, NO<sub>x</sub> lifetime, NO<sub>x</sub> scaling factor, and VCD thickness; all errors were within 20% of their reference emissions. We additionally quantified uncertainties introduced by ERA5 wind data using the spread of its wind field 10-member ensemble to perturb 2020 NO<sub>x</sub> emissions. The results show small changes in raw NO<sub>x</sub> emission (<4%; Table S1 and Figure S3 in Supporting Information S1), well within Dix et al. (2022) estimates. An approximately −23% bias in TROPOMI tropospheric NO<sub>2</sub> measurements (van Geffen et al., 2022) would result in emissions underestimation of the same order. Random error in annual NO<sub>x</sub> emissions, calculated from their spread in a region without significant sources (i.e., away from cities, mines, and industries; −12.5°N 26.5°E to −13.5°N 27.5°E), is ~0.1 kg km<sup>−2</sup> hr<sup>−1</sup>.

#### 4. Results

Six distinct point sources are clearly visible in the mean 2019–2022 TROPOMI NO<sub>2</sub> VCD map (Figure 1 and Figure S4 in Supporting Information S1). Four of the point sources correspond to large copper (Sentinel, a.k.a. Trident; Lumwana; Kansanshi) or copper-cobalt (Kolwezi and adjacent Katanga) open-pit mines. The remaining two point sources coincide with cities (Lubumbashi and Ndola) where we infer that high-emission industrial activities take place, as explained later in this Section. Latitudinal profiles of mean annual VCD across each point source (Figure 1) show that background NO<sub>2</sub> remains nearly constant year to year while the point sources (well defined, narrow peaks of fixed location) vary in magnitude. TROPOMI emission results (Table 1 and Figure S5 in Supporting Information S1) reinforce these observations. TROPOMI-derived NO<sub>x</sub> mostly increased with time at all the point sources but one, Ndola, where background-removed emissions decreased by >70% between 2019 and 2022.

To understand these inter-annual trends in NO<sub>x</sub> emissions, we compared background-removed TROPOMI-derived emissions to mine production data where available (Table 1 and Figure 2). Most of the energy consumed in copper or copper-cobalt mining, including electricity, is generated by diesel fuel combustion. Mining equipment consumes ~60% of the total energy; comminution ~36%; flotation, filtering, and drying ~4% (Allen, 2021). Limited data relevant to energy consumption is provided in mining company reports; we found the best proxy for energy (i.e., diesel) consumed to be amount of ore and waste mined. Panels b, c, and d in Figure 2 show strong positive correlation between annual values of total ore plus waste mined versus NO<sub>x</sub> emissions for the Sentinel, Lumwana, and Kansanshi mines ( $R = 0.82, 0.73, \text{ and } 0.81$ , respectively). Amount of copper produced (highly dependent on ore grade, among other factors, and thus, a less-desirable proxy) was used for the Kolwezi-Katanga mines (Figure 2a) for lack of ore and waste data ( $R = 0.83$ ).

The remaining two point sources coincide with some of the largest cities in the study area: Lubumbashi (DRC, population  $>2.6 \times 10^6$ ) and Ndola (Zambia, population  $>0.5 \times 10^6$ ). To discard the hypothesis that their emissions are due to urban activity alone, we quantified NO<sub>x</sub> emissions for two additional cities of similar size: Mbuji-Mayi (DRC, population  $>2.7 \times 10^6$ ), a remote and isolated enclave, despite its large population, located 750 km northwest of Lubumbashi; and Kitwe (Zambia, population  $>0.7 \times 10^6$ ), 50 km northwest of Ndola (labeled g in Figure 1 map). (Population data are for 2022 urban areas, Population Stat, 2023.) The results (Figure 1, Table S2, and Figure S6 in Supporting Information S1) show that neither the magnitude of VCD or emissions, the spatial extent of the plumes, or the temporal emission trends from Lubumbashi and Ndola can be explained by urban activity alone. Background-removed NO<sub>x</sub> emissions from Lubumbashi are higher than those from Mbuji-Mayi by approximately 90%, even though the population of the former is lower by 2%. Similarly, while its population is lower by 27%, emissions from Ndola surpass those from Kitwe by 40%–80%, depending on the year, and display inter-annual variations which do not correlate with changes in population. These findings are consistent with our hypothesis that emissions from Lubumbashi and Ndola are not the result of urban activity alone. We researched other possible origins for the excess emissions observed at these two point sources.

We hypothesize that Lubumbashi's high NO<sub>x</sub> emissions are due to reprocessing of the Lubumbashi slag heap: a  $14.5 \times 10^6$  tonne hill of mining residue located inside the city, resulting from metallurgical activity between 1924 and 1992 (Peša, 2022). Copper, cobalt, and zinc are extracted from the slag heap by La Société Congolaise du Terril de Lubumbashi (STL, 2000-present). Reports from the local press attest to the pollution resulting from the operation (Africa Intelligence, 2021). Figure 2e shows annual background-removed TROPOMI-derived NO<sub>x</sub> emissions; because production data is incomplete (STL, 2023; The Carter Center, 2023), emissions and mining-related activity cannot be compared in this case.

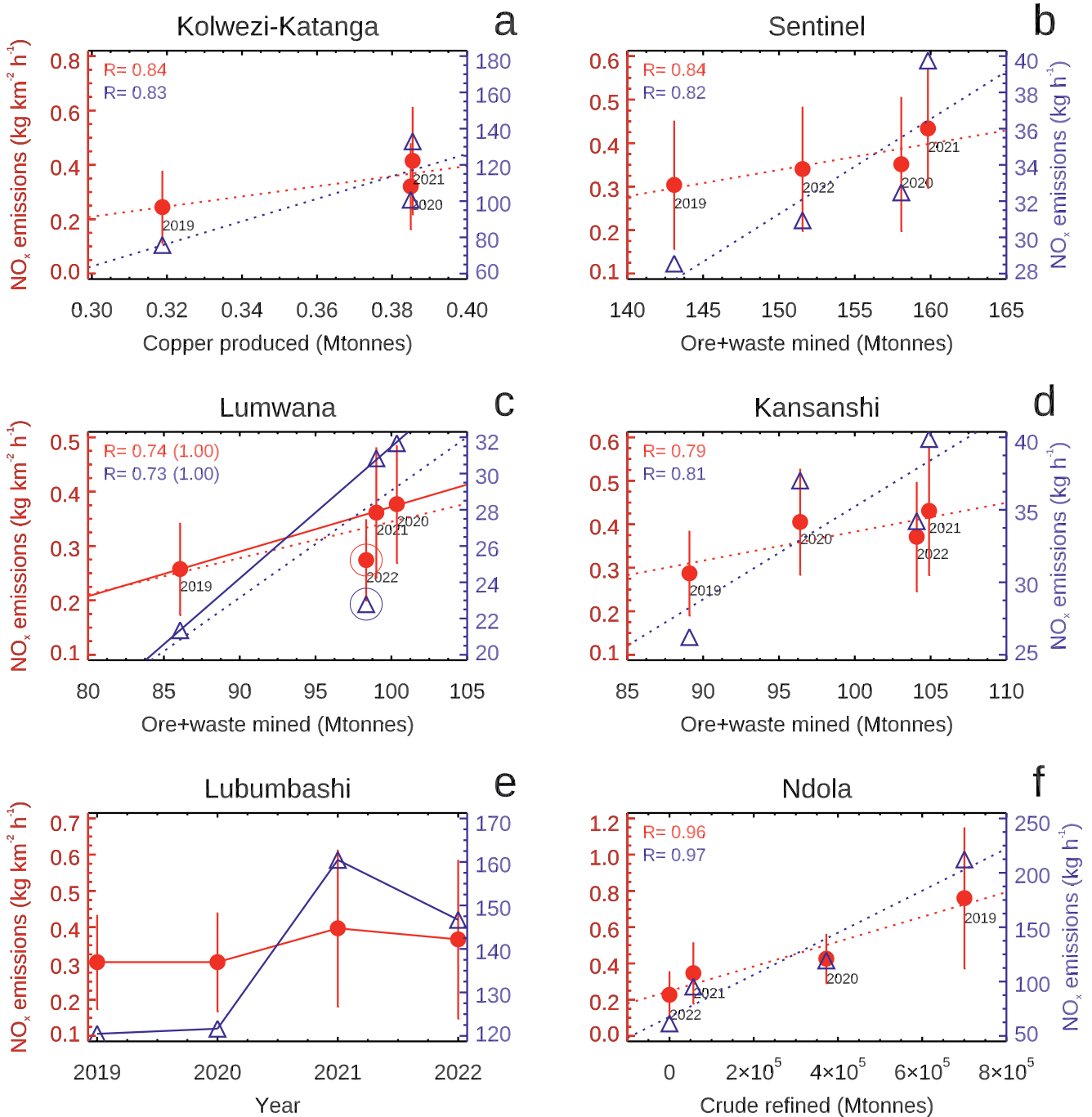
**Table 1**  
*Production and NO<sub>x</sub> Emissions for the Six Copperbelt Point Sources*

		2019	2020	2021	2022
Kolwezi <sup>a</sup> , Katanga <sup>b</sup>	Ore, Waste	–, –	–, –	–, –	–, –
	Copper	84.3, 234.5	114.3, 270.7	121.1, 264.4	–, 220.1
	Emissions	0.24 (0.13)	0.32 (0.16)	0.41 (0.20)	0.55 (0.23)
	Background	0.30 (0.11)	0.30 (0.13)	0.30 (0.13)	0.34 (0.13)
	Integrated emissions	75.79	100.75	132.98	172.23
	Inventory	0.04	0.04	0.04	–
Sentinel <sup>c</sup>	Ore, Waste	50,263, 92,826	60,098, 97,970	57,380, 102,445	56,219, 95,335
	Copper	220.006	251.216	232.688	242.451
	Emissions	0.30 (0.15)	0.35 (0.15)	0.43 (0.14)	0.34 (0.14)
	Background	0.27 (0.09)	0.29 (0.10)	0.27 (0.10)	0.31 (0.10)
	Integrated emissions	28.55	32.48	39.75	30.94
	Inventory	0.02	0.02	0.02	–
Lumwana <sup>d</sup>	Ore, Waste	23,230, 62,837	26,880, 73,480	33,510, 65,499	20,277, 78,063
	Copper	107.955	125.191	109.769	121.109
	Emissions	0.26 (0.09)	0.38 (0.11)	0.36 (0.12)	0.27 (0.08)
	Background	0.27 (0.09)	0.29 (0.10)	0.28 (0.09)	0.31 (0.09)
	Integrated emissions	21.35	31.67	30.84	22.79
	Inventory	0.04	0.04	0.04	–
Kansanshi <sup>c</sup>	Ore, Waste	36,325, 52,768	34,423, 61,972	35,142, 69,758	28,205, 75,878
	Copper	232.243	221.487	202.159	146.282
	Emissions	0.29 (0.10)	0.41 (0.12)	0.43 (0.15)	0.37 (0.13)
	Background	0.29 (0.10)	0.30 (0.11)	0.29 (0.10)	0.32 (0.10)
	Integrated emissions	26.22	37.02	39.88	34.21
	Inventory	0.09	0.09	0.09	–
Lubumbashi <sup>e</sup>	Throughput	–	–	255.229	–
	Emissions	0.30 (0.13)	0.30 (0.14)	0.40 (0.22)	0.37 (0.22)
	Background	0.33 (0.10)	0.34 (0.11)	0.33 (0.11)	0.34 (0.10)
	Integrated emissions	120.48	121.66	160.46	146.69
	Inventory	0.30	0.30	0.30	–
Ndola <sup>f</sup>	Throughput	700.277	372.384	56.672	0 <sup>g</sup>
	Emissions	0.76 (0.39)	0.43 (0.14)	0.35 (0.17)	0.23 (0.13)
	Background	0.27 (0.11)	0.28 (0.11)	0.27 (0.11)	0.30 (0.11)
	Integrated emissions	212.28	119.34	95.35	61.48
	Inventory	0.23	0.23	0.23	–

*Note.* Ore, waste, and copper produced are in kt. Throughput (slag processed in Lubumbashi, crude refined in Ndola) are in kt. Emissions and emissions integrated over the horizontal extent of the point source's plume have been background-removed. Emissions, background values, and their standard deviation (in parenthesis) are in kg km<sup>-2</sup> hr<sup>-1</sup>. Integrated emissions are in kg h<sup>-1</sup>.

<sup>a</sup>Zijin (2023). <sup>b</sup>Glencore (2023). <sup>c</sup>First Quantum (2023a). <sup>d</sup>Barrick (2023). <sup>e</sup>STL (2023). <sup>f</sup>Mwila et al. (2022). <sup>g</sup>Inactive.

The most plausible source for the excess emissions in Ndola is the INDENI petroleum refinery plant, located inside the city. Inactive since late 2021, its declining production values (Mwila et al., 2022) match well the TROPOMI-derived NO<sub>x</sub> emissions ( $R = 0.97$ , Figure 2f). Annual NO<sub>x</sub> emissions calculated for Ndola (and Lubumbashi as well) include emissions from industrial activities as well as from regular urban activities (e.g., traffic). The INDENI petroleum refinery in Ndola winding down its operations in late 2021 grants us an opportunity



**Figure 2.** TROPospheric Monitoring Instrument-derived, background-removed NO<sub>x</sub> emissions versus production, except (e), where production data is unavailable. Red circles: mean emission values with standard deviation shown as vertical lines. Blue triangles: emission values integrated over the horizontal extent of the point source. (c) Solid fit lines and *R* values in parenthesis exclude 2022 data; see text for details.

to estimate the relative size of emissions from other sources (urban activities) in that city, holding other factors constant: approximately 60 kg hr<sup>-1</sup> in 2022, which represents less than one third of total 2019 emissions and about half of total emissions in 2020.

The six Copperbelt NO<sub>x</sub> emission point sources do not coincide with SO<sub>2</sub> enhancements, as shown by the map of mean TROPOMI SO<sub>2</sub> VCD values for the period between January 2019 and July 2022 (Figure S7 in Supporting Information S1). This is despite the fact that some of them either include a smelter (Kansanshi, First



Quantum, 2023a) or have one nearby (Lualaba, 40 km southeast of Kolwezi; Ivanhoe Mines, 2021). Figure S7 in Supporting Information S1 does show SO<sub>2</sub> enhancements elsewhere: collocated with the Hwange coal power plant (Zimbabwe), the Selous smelter (Zimbabwe), and the Chingola and Mufulira smelters (Zambia). The lack of enhanced SO<sub>2</sub> at some sites could indicate either very low SO<sub>2</sub> amounts or low observational sensitivity. TROPOMI SO<sub>2</sub> detection depends on observation conditions. Generally, sites with low slant column density (SCD) noise and high measurement sensitivity (high air mass factor, or AMF) have better detection limits (Theys et al., 2021). Time series of SCD error and AMF (Figure S8 in Supporting Information S1) indicate that observation conditions at Kansanshi and Lualaba (the two smelters without SO<sub>2</sub> enhancements) are as good or better than those at Hwange, Selous, and Chingola/Mufulira (with SO<sub>2</sub> enhancements). Lack of SO<sub>2</sub> enhancements over Kansanshi and Lualaba is consistent with the use of technologies to capture and convert sulfur oxides released from the ore during smelting into sulfuric acid, a commercial byproduct (Hocking, 2005; Ialongo et al., 2018). The use of such technologies in the Kansanshi and Lualaba smelters has been documented by the mining companies involved (First Quantum, 2023b; Gray et al., 2020; Wang, 2020). The Kansanshi smelter produced on average  $1,240 \pm 19$  kt y<sup>-1</sup> of sulfuric acid during the 2019–2022 period (First Quantum, 2023a), equivalent to  $806 \pm 12$  kt y<sup>-1</sup> of SO<sub>2</sub> processed. Production from the Lualaba smelter has been reported to be 240 kt y<sup>-1</sup> of sulfuric acid and 30 kt y<sup>-1</sup> of liquid SO<sub>2</sub> (Wang, 2020), equivalent to 186 kt y<sup>-1</sup> of SO<sub>2</sub> processed. Those production figures are much higher (100 and 23 times higher, respectively) than TROPOMI's 8 kt y<sup>-1</sup> detection limit (Theys et al., 2021).

Anthropogenic emissions from the inventory were compared to TROPOMI-derived emissions from our six point sources as follows. Monthly inventory emissions from all sectors were aggregated, excluding agricultural and road transportation, which would be part of the background over our point sources (see Supporting Information S1 for additional details). Annual inventory means were calculated and compared to their background-removed TROPOMI counterparts (Table 1 and Figure S9 in Supporting Information S1). The inventory underpredicts emissions for all the mines (by 70%–96%) and from Ndola, the site on an oil refinery (by 35%–70%); it provides mixed results for Lubumbashi, the slag heap reprocessing site (inventory lower by 2%–24%). Even though inventory emissions are not constant along time, they do not capture the annual trends identified in TROPOMI-derived emissions, which are well correlated with annual mine production (Kolwezi-Katanga, Sentinel, Lumwana, Kansanshi) and oil refinery production (Ndola).

## 5. Discussion and Conclusions

Understanding the environmental effects of high-impact minerals extraction and processing is of great importance (Hund et al., 2020). This is particularly relevant for African regions where mining and other related industrial activities proliferate without sufficient air quality monitoring and often in close proximity to—or even inside of—population centers, as is the case in the Copperbelt mining region. Previous studies showed that NO<sub>2</sub> enhancements associated with mining could be observed using satellite data. Labzovskii et al. (2022) reported NO<sub>2</sub> from coal at basin scale using OMI data. TROPOMI allowed detecting NO<sub>2</sub> enhancements from large (~60 × 80 km) oil sand deposits (Griffin et al., 2019), as well as from large coal basins, copper mines, and gold mines (Goldberg et al., 2021). Dix et al. (2020) analyzed trends in OMI and TROPOMI NO<sub>2</sub> VCD from oil and gas production at basin scale (~200 × 200 km) and compared those with inventory data. NO<sub>x</sub> emissions from areal sources (corresponding to basin-scale oil and gas production) and point sources (from gas processing plants) were quantified by Dix et al. (2022).

In this study we have quantified for the first time NO<sub>x</sub> emissions from point sources corresponding to individual mines and one oil refinery, despite high background values from biomass burning, soils, and lightning (Table 1); this allows for the attribution of emissions to specific mines or industrial sites. As a reference, 2019 TROPOMI-derived NO<sub>x</sub> emissions from the Ndola oil refinery (212.28 kg hr<sup>-1</sup>) are similar to TROPOMI NO<sub>x</sub> emissions from the Intermountain power plant (194.40 kg hr<sup>-1</sup>), one of the top 10 2019 NO<sub>x</sub> emitters in the USA (Beirle et al., 2021).

We have analyzed the point sources with the highest mean annual TROPOMI-derived emissions in the Copperbelt. We show a string of NO<sub>2</sub> enhancements along the Ndola-Lubumbashi-Kolwezi corridor (Figure 1) where relatively smaller copper/cobalt mining operations, both industrial and artisanal, exist. Future work should explore the detection limits of this method by analyzing some of these other NO<sub>2</sub> enhancements. Beirle et al. (2019, 2021) reported a NO<sub>x</sub> detection limit of 0.03 kg s<sup>-1</sup> (108 kg hr<sup>-1</sup>) for ideal conditions when applying their iterative peak

fitting algorithm to emissions obtained with the divergence method. Dix et al. (2022) reported  $\text{NO}_x$  point source emissions well below that limit ( $0.7 \text{ t day}^{-1} = 29.17 \text{ kg hr}^{-1}$ ). The smallest  $\text{NO}_x$  point source reported here emits  $21.35 \text{ kg hr}^{-1}$ . Refinements in the divergence calculation, longer/more targeted time integrations, and improvements in background estimates, among others, may result in even lower  $\text{NO}_x$  detection limits.

Furthermore, we have shown strong positive correlations between annual  $\text{NO}_x$  emissions from single point sources and the annual production of individual mines as well as one oil refinery (Figure 2). Our results indicate that  $\text{NO}_x$  trend analysis could be used to predict mine production and refinery throughput, among others, before companies release their reports or in lieu of these reports in case of non-publicly traded companies, which are not required to publish their activity data. These correlations are, however, mine-dependent, and cannot be extrapolated from mine to mine; differences in ore grades and equipment fuel efficiency are probably the main causes. For example, lower-than-expected 2022 emissions from Lumwana, which reduced  $R$  from 1.00 (for 2019–2021) to 0.73 (for 2019–2022) (Figure 2c), can be traced to a new fleet of trucks and shovels commissioned in 2021 (Barrick, 2023) and in operation during 2022 (Lusaka Times, 2022). Insufficient emissions from mines claiming high production could be indicative of production from a different source. Thus, joint analyses of satellite-derived mine  $\text{NO}_x$  emissions versus reported mine production data may be useful for improving traceability of minerals extracted in conflict areas. This is an important issue highlighted in the most recent releases of the United Nations Yearbook (United Nations, 2019, 2022) and should be the subject of future work.

Ground  $\text{NO}_x$  emission measurements were unavailable; thus, we compared TROPOMI-derived  $\text{NO}_x$  emissions to CAMS-GLOB-ANT v5 inventory data. Inventory values are lower than their TROPOMI counterparts for all the mines analyzed as well as for Ndola, the site of an oil refinery, and (to a lesser degree) for Lubumbashi, the slag heap reprocessing site (Figure S9 in Supporting Information S1). The inventory does not represent well annual trends in TROPOMI emissions which are consistent with mine/oil refinery annual production data. The remoteness of the region, lack of field data, and relatively small size of the point sources may explain at least in part these discrepancies. Bottom-up inventories contain large uncertainties caused by inaccurate emission factors and activity rates; as a result, their representation of spatial and temporal variability is generally poor (Miyazaki et al., 2017).  $\text{NO}_x$  emissions derived from satellite measurements could improve the overall magnitude and temporal (seasonal, inter-annual) trends in inventory emissions, as proposed by Liu et al. (2022) and references therein. They could also be used to refine regional emission factors, which are not well defined for Africa.

We have also identified  $\text{SO}_2$  enhancements collocated with smelters and a coal power plant elsewhere, but none collocated with our Copperbelt  $\text{NO}_x$  point sources (Figure S7 in Supporting Information S1), some of which either include a smelter (Kansanshi) or have one nearby (Lualaba, near Kolwezi mine). TROPOMI observation conditions alone cannot explain the lack of  $\text{SO}_2$  enhancements over those two smelters. The companies operating the Kansanshi and Lualaba smelters report the amount of sulfuric acid (a byproduct used in mining-related processes and/or commercialized) resulting from the capture and conversion of sulfur oxides released from the ore during smelting. The amount of  $\text{SO}_2$  that would be released from either of these two smelters if capture techniques were not applied would far surpass TROPOMI's  $\text{SO}_2$  detection limit. These lines of evidence are consistent with the successful use of technologies for  $\text{SO}_2$  capture at the Kansanshi and Lualaba smelters.

Because the  $\text{NO}_x$  emissions analyzed here result from the combustion of fossil fuels by machinery (e.g., trucks, crushers, generators) extensively used in mining operations, these results are relevant to mining in general, regardless of the resource mined. They are also relevant to oil refineries, as shown in this study and (we hypothesize) to fossil-fuel intensive industries in general. These findings show that TROPOMI can be used to evaluate the effects on air quality of emissions from mining/refining activities at local scale; to attribute emissions to specific mines, refineries, etc.; and to detect and measure temporal changes in emissions potentially indicative of trends in production from individual mining/refining sites. This is of great importance in regions lacking local air quality monitoring, currently underestimated in emission inventories, and where mining and other industrial activities are increasing rapidly, in some cases without sufficient transparency and public accountability.

### Data Availability Statement

Atmospheric data available as follows. TROPOMI  $\text{NO}_2$  data (L2  $\text{NO}_2$ ) are available via the ESA's S-5P Pre-Ops interface (<https://scihub.copernicus.eu/>) using the credentials given there. TROPOMI  $\text{SO}_2$  COBRA data: <https://distributions.aeronomie.be/?menu=68c9f961bc294141c215e3d64a6ae282#>. ERA5 data:

<https://doi.org/10.24381/cds.f17050d7> (on single levels) and <https://doi.org/10.24381/cds.bd0915c6> (on pressure levels). CAMS-GLOB-ANT inventory data are available via the <https://eccad.sedoo.fr/> interface following the instructions given there to create a free access account.

Mining production data available from mining company reports as follows. Reports from First Quantum Minerals Ltd. (Sentinel, Kansanshi) and Barrick Gold Corporation (Lumwana) are available via the SEDAR (System for Electronic Document Analysis and Retrieval) interface ([https://www.sedar.com/search/search\\_en.htm](https://www.sedar.com/search/search_en.htm)) following the instructions provided there. Reports from Zijin Mining (Kolwezi): <https://www.zijinmining.com/upload/file/2020/09/14/9c97a89f8e9c4c59a13f2404f3bb1096.pdf> (2019), <https://www.zijinmining.com/upload/file/2021/06/09/538a46cc4831452e97b30cae55c9cf97.pdf> (2020), <https://www.zijinmining.com/upload/file/2022/06/20/771c971d76154257882f58ed03643c07.pdf> (2021), 2022 annual report not available at the time of writing. Reports from Glencore (Katanga): <https://www.glencore.com/.rest/api/v1/documents/5a08fe1942f92d-f7f2301ac3681e23aa/glen-2019-annual-report-interactive.pdf> (2019), [https://www.glencore.com/.rest/api/v1/documents/3505497f3cb94b24f0c79f5ba32b293b/Glencore\\_AR20\\_Interactive+%281%29.pdf](https://www.glencore.com/.rest/api/v1/documents/3505497f3cb94b24f0c79f5ba32b293b/Glencore_AR20_Interactive+%281%29.pdf) (2020), <https://www.glencore.com/.rest/api/v1/documents/ce4fec31fc81d6049d076b15db35d45d/GLEN-2021-annual-report.pdf> (2021), <https://www.glencore.com/.rest/api/v1/documents/ded10fa92974aa388a43aa9f86f483e9/GLEN-2022-Annual-Report.pdf> (2022).

ERA5 data are produced by C3S and CAMS. Contains modified information from C3S and CAMS (2019–2021). Neither the European Commission nor ECMWF is responsible for any use that may be made of the Copernicus information data contained in this study.

#### Acknowledgments

SMA thanks William Atkinson for sharing his deep knowledge of minerals and mining, Carol Atkinson for her insights and inspiring curiosity, Louisa Emmons for advice regarding models, David Edwards and Bill Randel for NCAR in-house comments. This paper benefited from constructive comments from three anonymous reviewers and careful editorial work by Christopher Cappa. This material is based upon work supported by the National Center for Atmospheric Research, which is a major facility sponsored by the National Science Foundation under Cooperative Agreement Nos. 1852977 and AGS-1755088. The KNMI contributions to this research have been funded by the Netherlands Space Office (NSO), as part of the TROPOMI Science Contract.

#### References

- Africa Intelligence. (2021). Lubumbashi slag heap locals fume over pollution. Retrieved from <https://www.africaintelligence.com/central-africa/2021/05/25/lubumbashi-slag-heap-locals-fume-over-pollution,109668540-art>
- Allen, M. (2021). Mining energy consumption 2021. Retrieved from <https://www.ceecethefuture.org/resources/mining-energy-consumption-2021>
- Atibu, E. K., Devarajan, N., Laffite, A., Giuliani, G., Salumu, J. A., Muteb, R. C., et al. (2016). Assessment of trace metal and rare earth elements contamination in rivers around abandoned and active mine areas. The case of Lubumbashi River and Tshamilemba Canal, Katanga, Democratic Republic of the Congo. *Chemie der Erde-Geochemistry*, 76(3), 353–362. <https://doi.org/10.1016/j.chemer.2016.08.004>
- Barrick (2023). Annual reports. Retrieved from <https://www.barrick.com/English/investors/default.aspx>
- Beirle, S., Boersma, K. F., Platt, U., Lawrence, M. G., & Wagner, T. (2011). Megacity emissions and lifetimes of nitrogen oxides probed from space. *Science*, 333(6050), 1737–1739. <https://doi.org/10.1126/science.1207824>
- Beirle, S., Borger, C., Doerner, S., Eskes, H., Kumar, V., de Laat, A., & Wagner, T. (2021). Catalog of NO<sub>x</sub> emissions from point sources as derived from the divergence of the NO<sub>2</sub> flux for TROPOMI. *Earth System Science Data*, 13(6), 2995–3012. <https://doi.org/10.5194/essd-13-2995-2021>
- Beirle, S., Borger, C., Dörner, S., Li, A., Hu, Z., Liu, F., et al. (2019). Pinpointing nitrogen oxide emissions from space. *Science Advances*, 5(11), eaax9800. <https://doi.org/10.1126/sciadv.aax9800>
- BIRA-IASB. (2021). Global map of nitrogen dioxide (NO<sub>2</sub>). Retrieved from [https://uv-vis.aeronomie.be/data/tropomi\\_posters/posterTROPOMI\\_NO2\\_2018\\_2020.pdf](https://uv-vis.aeronomie.be/data/tropomi_posters/posterTROPOMI_NO2_2018_2020.pdf)
- Carn, S. A., Krueger, A. J., Krotkov, N. A., Yang, K., & Levelt, P. F. (2007). Sulfur dioxide emissions from Peruvian copper smelters detected by the Ozone Monitoring Instrument. *Geophysical Research Letters*, 34(9), L09801. <https://doi.org/10.1029/2006GL029020>
- de Foy, B., & Schauer, J. J. (2022). An improved understanding of NO<sub>x</sub> emissions in South Asian megacities using TROPOMI NO<sub>2</sub> retrievals. *Environmental Research Letters*, 17(2), 024006. <https://doi.org/10.1088/1748-9326/ac48b4>
- Dix, B., de Bruin, J., Roosenbrand, E., Vlemmix, T., Francoeur, C., Gorchov-Negron, A., et al. (2020). Nitrogen oxide emissions from US oil and gas production: Recent trends and source attribution. *Geophysical Research Letters*, 47(1), e2019GL085866. <https://doi.org/10.1029/2019GL085866>
- Dix, B., Francoeur, C., Li, M., Serrano-Calvo, R., Levelt, P. F., Veefkind, J. P., et al. (2022). Quantifying NO<sub>x</sub> emissions from US oil and gas production regions using TROPOMI NO<sub>2</sub>. *ACS Earth and Space Chemistry*, 6(2), 403–414. <https://doi.org/10.1021/acsearthspacechem.1c00387>
- Eskes, H., & Eichmann, K.-U. (2021). *S-5P Mission Performance Centre nitrogen dioxide (L2\_NO2\_\_\_) readme (technical report nos. S5P-MPC-KNMI-PRF-NO2, 2.1, 02.03.01, 2021-11-17)*. Netherlands Institute for Space Research (SRON). Retrieved from <https://sentinels.copernicus.eu/documents/247904/3541451/Sentinel-5P-Nitrogen-Dioxide-Level-2-Product-Readme-File>
- Eskes, H., van Geffen, J., Boersma, F., Eichmann, K.-U., Apituley, A., Pedernana, M., et al. (2022). *Sentinel-5 Precursor/TROPOMI level 2 product user manual nitrogen dioxide (technical report nos. S5P-KNMI-L2-0021-MA, 4.1.0, 2.4.0, 2022-07-11)*. Netherlands Institute for Space Research (SRON). Retrieved from <https://sentinel.esa.int/documents/247904/2474726/Sentinel-5P-Level-2-Product-User-Manual-Nitrogen-Dioxide.pdf>
- Fioletov, V., McLinden, C. A., Griffin, D., Abboud, I., Krotkov, N., Leonard, P. J. T., et al. (2023). Version 2 of the global catalogue of large anthropogenic and volcanic SO<sub>2</sub> sources and emissions derived from satellite measurements. *Earth System Science Data*, 15(1), 75–93. <https://doi.org/10.5194/essd-15-75-2023>
- Fioletov, V., McLinden, C. A., Griffin, D., Theys, N., Loyola, D. G., Hedelt, P., et al. (2020). Anthropogenic and volcanic point source SO<sub>2</sub> emissions derived from TROPOMI on board Sentinel-5 Precursor: First results. *Atmospheric Chemistry and Physics*, 20(9), 5591–5607. <https://doi.org/10.5194/acp-20-5591-2020>
- Fioletov, V., McLinden, C. A., Krotkov, N., Yang, K., Loyola, D. G., Valks, P., et al. (2013). Application of OMI, SCIAMACHY, and GOME-2 satellite SO<sub>2</sub> retrievals for detection of large emission sources. *Journal of Geophysical Research-Atmospheres*, 118(19), 11399–11418. <https://doi.org/10.1002/jgrd.50826>
- First Quantum. (2023a). Annual reports. Retrieved from <https://www.first-quantum.com/English/investors/financial-information/default.aspx>
- First Quantum. (2023b). Kansanshi smelter. Retrieved from <https://www.first-quantum.com/English/our-operations/default.aspx#module-operation--kansanshi>

- Glencore. (2023). Annual reports. Retrieved from <https://www.glencore.com/publications>
- Goldberg, D. L., Anenberg, S. C., Kerr, G. H., Moheg, A., Lu, Z., & Streets, D. G. (2021). TROPOMI NO<sub>2</sub> in the United States: A detailed look at the annual averages, weekly cycles, effects of temperature, and correlation with surface NO<sub>2</sub> concentrations. *Earth's Future*, 9(4), e2020EF001665. <https://doi.org/10.1029/2020EF001665>
- Goldberg, D. L., Lu, Z., Streets, D. G., de Foy, B., Griffin, D., McLinden, C. A., et al. (2019). Enhanced capabilities of TROPOMI NO<sub>2</sub>: Estimating NO<sub>x</sub> from North American cities and power plants. *Environmental Science and Technology*, 53(21), 12594–12601. <https://doi.org/10.1021/acs.est.9b04488>
- Granier, C., Darras, S., Denier van der Gon, H., Doubalova, J., Elguindi, N., Galle, B., et al. (2019). *The Copernicus atmosphere monitoring Service global and regional emissions (technical report)*. Copernicus Atmosphere Monitoring Service (CAMS). <https://doi.org/10.24380/d0bn-kx16>
- Gray, D., Lawlor, M., & Briggs, A. (2020). *Kansanshi operations, North West Province, Zambia (technical report no. NI 43-101)*. First Quantum Minerals Ltd. Retrieved from [https://s24.q4cdn.com/821689673/files/doc\\_downloads/2021/NI-43-101/NI-43-101-Technical-Report-Kansanshi.pdf](https://s24.q4cdn.com/821689673/files/doc_downloads/2021/NI-43-101/NI-43-101-Technical-Report-Kansanshi.pdf)
- Griffin, D., Zhao, X., McLinden, C. A., Boersma, F., Bourassa, A., Dammers, E., et al. (2019). High-resolution mapping of nitrogen dioxide with TROPOMI: First results and validation over the Canadian Oil Sands. *Geophysical Research Letters*, 46(2), 1049–1060. <https://doi.org/10.1029/2018GL081095>
- Gulley, A. L. (2022). One hundred years of cobalt production in the Democratic Republic of the Congo. *Resources Policy*, 79, 103007. <https://doi.org/10.1016/j.resourpol.2022.103007>
- Hersbach, H., Bell, B., Berrisford, P., Hirahara, S., Horanyi, A., Muñoz-Sabater, J., et al. (2020). The ERA5 global reanalysis. *Quarterly Journal of the Royal Meteorological Society*, 146(730), 1999–2049. <https://doi.org/10.1002/qj.3803>
- Hocking, M. B. (2005). Ore enrichment and smelting of copper. In M. B. Hocking (Ed.), *Handbook of chemical technology and pollution control* (3rd ed., pp. 391–420). Academic Press. <https://doi.org/10.1016/B978-012088796-5/50016-8>
- Hund, K., LaPorta, D., Fabregas, T., Laing, T., & Drexhage, J. (2020). *Minerals for climate action: The mineral intensity of the clean energy transition*. The World Bank. Retrieved from <https://pubdocs.worldbank.org/en/961711588875536384/Minerals-for-Climates-Action-The-Mineral-Intensity-of-the-Clean-Energy-Transition.pdf>
- Ialongo, I., Fioletov, V., McLinden, C., Jafs, M., Krotkov, N., Li, C., & Tamminen, J. (2018). Application of satellite-based sulfur dioxide observations to support the cleantech sector: Detecting emission reduction from copper smelters. *Environmental Technology & Innovation*, 12, 172–179. <https://doi.org/10.1016/j.eti.2018.08.006>
- Ivanhoe Mines. (2021). Agreement signed with nearby Lualaba copper smelter to produce 99% blister copper in the Democratic Republic of Congo. Retrieved from <https://ivanhoemines.com/news/2021/kamoa-kakulas-off-take-agreements-signed-for-phase-1-blister-copper-and-copper-concentrate/>
- Kayembe-Kitenge, T., Lubala, T. K., Obadia, P. M., Chimusa, P. K., Nawej, C. K., Nkulu, C. B. L., et al. (2019). Holoprosencephaly: A case series from an area with high mining-related pollution. *Birth Defects Research*, 111(19), 1561–1563. <https://doi.org/10.1002/bdr2.1583>
- Krueger, A. (1983). Sighting of El Chichón sulfur dioxide clouds with the Nimbus 7 total ozone mapping spectrometer. *Science*, 220(4604), 1377–1379. <https://doi.org/10.1126/science.220.4604.1377>
- Labzovskii, L. D., Belikov, D. A., & Damiani, A. (2022). Spaceborne NO<sub>2</sub> observations are sensitive to coal mining and processing in the largest coal basin of Russia. *Scientific Reports*, 12(1), 12597. <https://doi.org/10.1038/s41598-022-16850-8>
- Leue, C., Wenig, M., Wagner, T., Klimm, O., Platt, U., & Jahne, B. (2001). Quantitative analysis of NO<sub>x</sub> emissions from Global Ozone Monitoring Experiment satellite image sequences. *Journal of Geophysical Research*, 106(D6), 5493–5505. <https://doi.org/10.1029/2000JD900572>
- Liu, F., Tao, Z., Beirle, S., Joiner, J., Yoshida, Y., Smith, S. J., et al. (2022). A new method for inferring city emissions and lifetimes of nitrogen oxides from high-resolution nitrogen dioxide observations: A model study. *Atmospheric Chemistry and Physics*, 22(2), 1333–1349. <https://doi.org/10.5194/acp-22-1333-2022>
- Lusaka Times. (2022). Barrick hoping to extend Lumwana mine to 2042. Retrieved from <https://www.lusakatimes.com/2022/10/31/barrick-hoping-to-extend-lumwana-mine-to-2042/>
- Miyazaki, K., Eskes, H., Sudo, K., Boersma, K. F., Bowman, K., & Kanaya, Y. (2017). Decadal changes in global surface NO<sub>x</sub> emissions from multi-constituent satellite data assimilation. *Atmospheric Chemistry and Physics*, 17(2), 807–837. <https://doi.org/10.5194/acp-17-807-2017>
- Mwila, A. M., Sinyenga, G., Buumba, S., Muyangwa, R., Mukelabai, N., Sikwanda, C., et al. (Eds.). (2022). *2021 energy sector report*. Retrieved from <https://www.erb.org.zm/wp-content/uploads/files/esr2021.pdf>
- Mwitwa, J., German, L., Muimba-Kankolongo, A., & Puntodewo, A. (2012). Governance and sustainability challenges in landscapes shaped by mining: Mining-forestry linkages and impacts in the Copper Belt of Zambia and the DR Congo. *Forest Policy and Economics*, 25, 19–30. <https://doi.org/10.1016/j.forpol.2012.08.001>
- Myhre, G., Shindell, D., Bréon, F.-M., Collins, W., Fuglestedt, J., Huang, J., et al. (Eds.). *Climate change 2013: The physical science basis. Contribution of working group I to the fifth assessment report of the intergovernmental panel on climate change* (pp. 659–740). Cambridge University Press. <https://doi.org/10.1017/CBO9781107415324.018>
- Peša, I. (2022). Mining, waste and environmental thought on the Central African Copperbelt, 1950–2000. *Environment and History*, 28(2), 259–284. <https://doi.org/10.3197/096734019X15755402985703>
- Pommier, M. (2022). Estimations of NO<sub>x</sub> emissions, NO<sub>2</sub> lifetime and their temporal variation over three British urbanised regions in 2019 using TROPOMI NO<sub>2</sub> observations. *Environmental Science-Atmospheres*, 3(2), 408–421. <https://doi.org/10.1039/d2ea00086e>
- Population Stat. (2023). World statistical data. Retrieved from <https://populationstat.com/>
- Richter, A., Begoin, M., Hilboll, A., & Burrows, J. P. (2011). An improved NO<sub>2</sub> retrieval for the GOME-2 satellite instrument. *Atmospheric Measurement Techniques*, 4(6), 1147–1159. <https://doi.org/10.5194/amt-4-1147-2011>
- Richter, A., Burrows, J., Nuss, H., Granier, C., & Niemeier, U. (2005). Increase in tropospheric nitrogen dioxide over China observed from space. *Nature*, 437(7055), 129–132. <https://doi.org/10.1038/nature04092>
- STL. (2023). Statistiques de production. Retrieved from <http://www.stlgcm.com/>
- The Carter Center. (2023). Mining royalty statistics for the province of H-Katanga/Cumulative 2021. Retrieved from <https://congominer.org/reports/>
- Theys, N. (2022). *S5P COBRA sulphur dioxide (L2\_SO2CBR\_) readme (technical report nos. S5P-BIRA-PRF-SO2CBR, 1.0.0, 2022-09-14)*. Royal Belgian Institute for Space Aeronomy (BIRA-IASB). Retrieved from [https://data-portal.s5p-pal.com/product-docs/so2cbr/S5P-BIRA-PRF-SO2CBR\\_1.1.pdf](https://data-portal.s5p-pal.com/product-docs/so2cbr/S5P-BIRA-PRF-SO2CBR_1.1.pdf)
- Theys, N., Fioletov, V., Li, C., De Smedt, I., Lerot, C., McLinden, C., et al. (2021). A sulfur dioxide COvariance-Based Retrieval Algorithm (COBRA): Application to TROPOMI reveals new emission sources. *Atmospheric Chemistry and Physics*, 21(22), 16727–16744. <https://doi.org/10.5194/acp-21-16727-2021>



- United Nations. (2019). *Yearbook of the United Nations, 2014* (Vol. 68). United Nations Department of Global Communications. Retrieved from <https://www.un.org/yearbook/>
- United Nations. (2022). *Yearbook of the United Nations, 2015* (Vol. 69). United Nations Department of Global Communications. Retrieved from <https://www.un.org/yearbook/>
- U.S. Bureau of Mines. (1992). *Minerals yearbook: Mineral industries of Africa 1990* (Vol. 3). U.S. Department of the Interior, Bureau of Mines. Retrieved from <https://digital.library.wisc.edu/1711.dl/M42DNFFQNI2X29B>
- U.S. Geological Survey. (2022). *Mineral commodity summaries 2022*. U.S. Geological Survey. <https://doi.org/10.3133/mcs2022>
- Van Brusselen, D., Kayembe-Kitenge, T., Mbuyi-Musanazayi, S., Kasole, T. L., Ngombe, L. K., Obadia, P. M., et al. (2020). Metal mining and birth defects: A case-control study in Lubumbashi, Democratic Republic of the Congo. *The Lancet Planetary Health*, 4(4), E158–E167. [https://doi.org/10.1016/S2542-5196\(20\)30059-0](https://doi.org/10.1016/S2542-5196(20)30059-0)
- van Geffen, J., Boersma, K. F., Eskes, H., Sneep, M., ter Linden, M., Zara, M., & Veefkind, J. P. (2020). S5P TROPOMI NO<sub>2</sub> slant column retrieval: Method, stability, uncertainties and comparisons with OMI. *Atmospheric Measurement Techniques*, 13(3), 1315–1335. <https://doi.org/10.5194/amt-13-1315-2020>
- van Geffen, J., Eskes, H., Compernelle, S., Pinardi, G., Verhoelst, T., Lambert, J.-C., et al. (2022). Sentinel-5P TROPOMI NO<sub>2</sub> retrieval: Impact of version v2.2 improvements and comparisons with OMI and ground-based data. *Atmospheric Measurement Techniques*, 15(7), 2037–2060. <https://doi.org/10.5194/amt-15-2037-2022>
- Veefkind, J. P., Aben, I., McMullan, K., Forster, H., de Vries, J., Otter, G., et al. (2012). TROPOMI on the ESA Sentinel-5 precursor: A GMES mission for global observations of the atmospheric composition for climate, air quality and ozone layer applications. *Remote Sensing of Environment*, 120(S1), 70–83. <https://doi.org/10.1016/j.rse.2011.09.027>
- Wang, R. (2020). CNMC-invested and constructed mining, copper smelting projects go into production. Retrieved from [http://en.sasac.gov.cn/2020/01/22/c\\_12660.htm](http://en.sasac.gov.cn/2020/01/22/c_12660.htm)
- World Health Organization. (2021). *WHO global air quality guidelines: Particulate matter (PM<sub>2.5</sub> and PM<sub>10</sub>), ozone, nitrogen dioxide, sulfur dioxide and carbon monoxide*. World Health Organization. Retrieved from <https://apps.who.int/iris/bitstream/handle/10665/345329/9789240034228-eng.pdf?sequence=1&isAllowed=y>
- Zhang, Y., Li, C., Krotkov, N. A., Joiner, J., Fioletov, V., & McLinden, C. (2017). Continuation of long-term global SO<sub>2</sub> pollution monitoring from OMI to OMPS. *Atmospheric Measurement Techniques*, 10(4), 1495–1509. <https://doi.org/10.5194/amt-10-1495-2017>
- Zijin. (2023). Annual reports. Retrieved from <https://www.zijinmining.com/investors/Annual-Reports.jsp>